Evaluating the reservoir properties of Nahr Umr Formation at Luhais oil field, southern Iraq using well logs data

Amna M. Handhal, Amjad AbdulZahra Hussein
Department of Geology, College of Science, University of Basra, Basra, Iraq
*Corresponding authors: Amna M. Handhal, e-mail: amna.handhal@uobasrah.edu.iq
Amjad AbdulZahra Hussein, e-mail: abdulaamjad3@gmail.com

Doi 10.29072/basjs.202028

Abstract

Nahr Umr formation in the oilfield of Luhais in southern Iraq is one of productive clastic reservoirs which formed during the secondary Alpine cycle. To cover the objectives of this study, twenty two wells were selected to evaluate the reservoir characteristics of the Nahr Umr formation in Luhais oilfield in southern Iraq. The petrophysical characteristics (Shale Volume (Vsh), Bulk volume hydrocarbon (BVH), Hydrocarbon saturation (Sh), Water saturation (Sw), thickness, Bulk water volume (BVW), porosity (φ) were calculated and interpreted using the Geolog software. The Nahr Umr Formation was divided into three main reservoir units based on their petrophysical properties, these units are: Upper Nahr Umr reservoir unit, Middle Nahr Umr reservoir unit and Lower Nahr Umr reservoir unit. It was found that the best reservoir units in terms of hydrocarbon saturation and production are the middle Nahr Umr reservoir unit.

Article inf.

Received: 07/5/2020

Accepted 28/6/2020

Published 31/8/2020

Keywords:

Nahr Umr, Luhais oil field, Petrophysical characteristics,

1. Introduction

The process of evaluation the petrophysical properties of petroleum reservoirs is a complex that requires analysis and integration of information of a different nature (qualitative and quantitative) and from different sources (seismic, surface, rock samples, well logs, laboratory tests). the petrophysical properties evaluation by well logs data is important in determining and evaluating hydrocarbon presence areas and plays main role in determining the production potential of petroleum reservoirs. In this study, many well logs (Gamma ray log (GR), Neutron log (NPHI), Density log (RHOB), Resistivity logs (Rxo, Ri, Rt) , Sonic log (Δt)) were used to interpretation the qualitative and quantitative properties of rocks, From the qualitative interpretation of the well logs data it can be determine the lithology, thickness, depth and correlation between the wells and description of facies relationship of the sedimentary environment. The properties of the reservoir are evaluated using the quantitative interpretation in addition to the assess the rock porosity (φ), permeability, volume of shale (Vsh), water saturation (Sw) , oil saturation (Sh), etc.

2. Study Area

The Luhias oil field is located in the Basra Governorate, close to the administrative borders of Nasiriyah Governorate, 105 km west of the Basra Governorate center and 100 km southwest of the giant North Rumaila oil field. The field is 20 km long and 5 km wide in the northern part of the field and 10 km wide in the southern part [1]. The shape of the structure appears to be amoebic as no specific axis is apparent for the structure (Fig. 1). From a tectonic point of view, the field is located in a formerly unstable shelf zone, the Zubair subzone [2], which is considered to be the southern part of the Mesopotamian zone, a Cenozoic foreland basin formed between the colliding Arabian and Iranian plates [3, 4, and 5]. The Zubair subzone is bordered on the north by the transverse (NE-SW) Takhadid Qurna fault and on the south by the transverse (NE SW) Al-Batin fault in the Basra district [3].

The region was probably uplifted during the Hercynian deformation that took place from Late Devonian through Middle Permian time, but subsequently subsided through Late Permian time [4]. Most of the oil fields in southern Iraq (including Luhais oil field) were formed as a result of the impact of the Arabian Plate with parts of the Iranian plate to the north and east during Oligocene time. The resulting compression affected the form of depositional layers in the basins along the northeastern edge of the Arabian Plate, including the Mesopotamian foreland

basin, resulting in broad folds that later became large oil traps [6]. It is also believed that the Luhais oil field formed along lineation developed during eruption of the Neoproterozoic–Cambrian (Infracambrian) Hormuz Salt Formation [7, 8], which continued through Jurassic time. The collision of Arabian and Iranian plates contributed to the final form of the field in Miocene-Pliocene time [9]. The Nahr Umr Formation, the target of this study, is a sandstone reservoir initially defined by Glynn Jones in 1948 from the Nahr Umr structure in southern Iraq [10] In its type area in southern Iraq, it comprises black shale interbedded with medium- to fine-grained sandstones with lignite, amber, and pyrite [11]. The sandstone is locally sealed by shales beneath the Mauddud Formation [12].

According to Dunnington et al. (1959) [13], a carbonate unit occurs locally in the upper part of Nahr Umr Formation in southern Iraq, pinching out to the west and south. The formation is up to 300 m thick and thins eastwards, becoming less sandy and more carbonate-rich toward Iraq [14]. The formation is Late Aptian–Albian in age, and depositional environments include alluvial to lower coastal plain to deltaic deposits with shallow-marine and aeolian influences [14]. Based on qualitative and quantitative interpretation of conventional well-log data, the Nahr Umr Formation can be divided into three reservoir units of sandstone with smaller amounts of interbedded shale, separated by two prominent shale layers, thereby dividing the formation into upper, middle, and lower reservoir units.

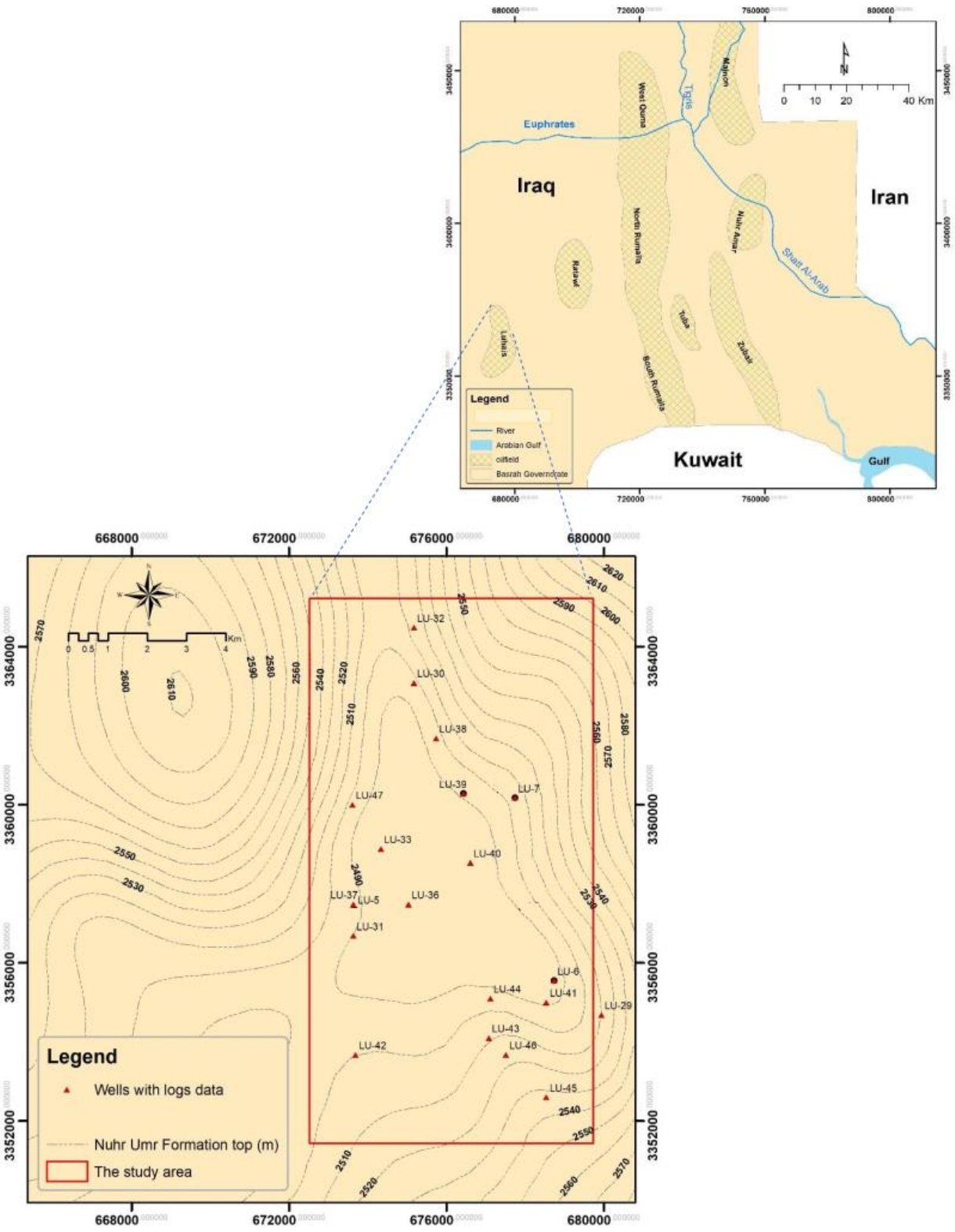

Fig. 1: Location of the study area in southeastern Iraq.

3. Methodology and materials

Computer processing interpretation (CPI) was intepretrd by Geolog software for estimate and petrophysical charachteristics and identifying reservoirs units based on well logs data (Caliper, Gamma ray log (GR), Resistivity (Rxo, Ri, Rt), Neutron log (NPHI), Density log (RHOB), Sonic log (Δt)) for wells (Lu- 005, Lu-006, Lu- 007, Lu-018, Lu-029, Lu-030, Lu-031, Lu-032, Lu-030, Lu- 033, Lu-036, Lu-037, Lu-038, Lu-039, Lu-040, Lu-041, Lu-042, Lu-043, Lu-044, Lu-045, Lu-046, Lu-047, Lu-048). To determine petrophysical charachteristics of the Nahr Umr formation. For estimating petrophysical charachteristics and identifying reservoirs units of Nahr Umr Formation as follows:

3.1 Determination of shale volume

The presence of shale in formation has significant effect on the petrophysical properties of the reservoir such as total porosity, effective porosity, permeability and water saturation. Its presence in oil reservoirs does not give an accurate assessment of the reservoir and a correct estimate of oil and gas reserves [15]. Therefore, it is necessary to calculate shale volume (V_{sh}) in formation. It was calculated by the GR log, which is the best in calculating of the shale volume (V_{sh}) by using equation [16]:

$$V_{sh} = 0.33 \times \left(2^{(2 \times I_{GR})} - 1\right) \quad (1)$$

To determine the shale volume (V_{sh}) we first calculate gamma ray index [16] from the following relationship:

$$I_{GR} = \frac{GR_{log} - GR_{matrix}}{GR_{shale} - GR_{matrix}} \quad (2)$$

with the values defined as follows:

GR_{log} = gamma ray reading of formation, API

GR_{matrix} = minimum gamma ray in clean sand or carbonate, API

GR_{shale} = maximum gamma ray in shale, API

Depending on the shale volume extracted from equation (3.1) for each well, the shale-free area where the value of V_{sh} is less than 10% is determined and the area containing the shale (unclean) at which the value of V_{sh} is greater or equal to 10%.

3.2 Determination of porosity

Porosity is an important characteristic of rock because it is a measure of hydrocarbon storage capacity [17]. It is defined as volume of voids to the total volume of the rock and is represented as percentage and is expressed by the following equation:

$$\text{Porosity\%} = \frac{Volume\ of\ voids}{Total\ volume\ of\ rock} * 100 \quad (3)$$

the common source to determine the porosity is well logs. Porosity may be calculated by an acoustic log (Δt log), a density log (RHOB log) and a neutron log (NPHI log), which is referred to as porosity logs.

A. Sonic log (Δt)

The sonic log responds to porosity arising from fractures and intergranular porosity [18]. The simplest relationship to measure the porosity of sonic log is the line relationship known as Wyllie time-average equation [19], which is used in clean depths.

$$\emptyset_s = \frac{\Delta t_{log} - \Delta t_{ma}}{\Delta t_f - \Delta t_{ma}} \quad (4)$$

where: $\emptyset_s$ = porosity derived from the sonic log

Δt_{log} = the wave transit interval in the formation is measured from then log recording directly, μs/ft

Δt_{ma} = matrix travel time (Sandstone 51 to 55.5), μs/ft

Δt_f = fluid travel time (Saline mud *185*& fresh mud 189), μs/ft.

In the zones where the shale is more than 10% (shaly zone), the Dresser atlas equation is used to remove the shale effect:

$$\emptyset_{sc} = \left[\frac{\Delta t_{log} - \Delta t_{ma}}{\Delta t_f - \Delta t_{ma}}\right] - \left[\frac{\Delta t_{sh} - \Delta t_{ma}}{\Delta t_f - \Delta t_{ma}}\right] * V_{sh} \quad (5)$$

where $\emptyset_{sc}$ = corrected porosity of shale effect

Δt_{sh} = shale travel time, μs/ft.

The presence of hydrocarbon causes an increase in Δt as well as increase in $\emptyset_s$, so Hilchie, 1978 suggested an equation to correct the effect of hydrocarbon as follows:

$$\emptyset_{sc} = \emptyset_s * Bhc \quad (6)$$

where $\emptyset_{sc}$ = porosity derived from the sonic log and corrected from the effect of hydrocarbons

Bhc = the coefficient of hydrocarbon effect is compensated by 0.9 for oil and 0.7 for gas.

B. Density log (RHOB)

The density log responds to density of electrons in the formation that are related to the total density [16]. Total density represents the density of the solid part of the formation and density of fluid present in the formation pores. Density log is one of the porosity logs where porosity can be calculated in the following equation [16]:

$$\emptyset_D = \frac{\rho_{ma} - \rho_b}{\rho_{ma} - \rho_f} \quad (7)$$

where: $\emptyset_D$ = Porosity derived from the density log

ρ_{ma} = matrix density (Sandstone 2.64 – 2.68), gm/cm^3

ρ_b = bulk density, gm/cm^3

ρ_f = fluid density (Salt mud 1.1), gm/cm^3.

in the zones the bearing to shale, the following formula is used to remove the shale effect[18]:

$$\emptyset_D = \left[\frac{\rho_{ma} - \rho_b}{\rho_{ma} - \rho_f}\right] - \left[\frac{\rho_{ma} - \rho_{sh}}{\rho_{ma} - \rho_f}\right] * V_{sh} \quad (8)$$

porosity can also be measured directly from the neutron log to shale-free depths. For the depths containing the shale, the following equation is used [20]:

$$\emptyset_{Nc} = \emptyset_N - (\emptyset_{N_{sh}} * V_{sh}) \quad (9)$$

where: $\emptyset_{Nc}$ = porosity derived from the neutron log and corrected from the shale effect

$\emptyset_N$ = Porosity derived from the neutron log

$\emptyset_{N_{sh}}$ = the neutron porosity of the shale in a formation.

Effective porosity can be determined by density and neutron for deep intervals containing less than 10% shale using the following equation [21]:

$$\emptyset_{N.D} = \frac{\emptyset_N - \emptyset_D}{2} \quad (10)$$

Where $\emptyset_{N.D}$ = effective porosity calculated from the density and neutron log for the zones of oil and gas bearing.

as for effective porosity in deep intervals with a shale content of more than 10% uses the following equation:

$$\emptyset_{N.D_c} = \frac{\emptyset_{N_c} - \emptyset_{D_c}}{2} \quad (11)$$

3.3 Determination of fluid saturation

Determination of fluid saturation mainly involves distinguishing between various fluid components (water and hydrocarbon) that fill the pores in the flushed zone and uninvaded zone. Water saturation is the most important step in the interpretation of logs. Water saturation in the uninvaded zone at depths where the shale content is less than 10% was determined using the following equation [22]:

$$S_w = \left[\frac{F * R_w}{R_t}\right]^{1/n} \quad (12)$$

where: S_w = water saturation of the uninvaded zone, fraction

F = formation factor of the reservoir

R_w = resistivity of formation water, Ω.m

R_t = true formation resistivity, Ω.m

n = saturation exponent [23]

In depths where shale content is more than 10%, water saturation is determined by the following equation [16]:

$$S_w = \left(\frac{0.4 * R_w}{\emptyset^2}\right) * \left[\sqrt{\left(\frac{V_{sh}}{R_{sh}}\right)^2 + \frac{5 * \emptyset^2}{R_t * R_w}} - \frac{V_{sh}}{R_{sh}}\right] \quad (13)$$

where R_{sh} = shale resistivity value in a formation, Ω.m

when porosity, permeability and formation water penetrate with drilling mud filtrate, the mud filtrate will replace the formation water.

Hydrocarbon saturation (S_h) is determined by the following equation [24]:

$$S_h = 1 - S_h \quad (14)$$

To apply the Archie's equations, it is necessary to clarify how to determine their variables:

A. Calculate the formation factor (F)

Archie, 1942 showed explained that resistivity of a formation 100% saturated with formation water is associated with the resistivity of water formation (R_w) through a constant called formation factor (f)

$$S_o = F * R_w \quad (15)$$

Also, Archie explained that the formation factor (F) is related to the porosity of the formation through the following equation:

$$F = \frac{a}{\emptyset^m} \quad (16)$$

where: m = cementation factor [23]

a = tortuosity factor

B. Determination the formation water resistivity (R_w) and mud filtrate resistivity (R_{mf})

R_w and R_{mf} are significant explanation coefficients for determining water saturation and hydrocarbon saturation by basic resistivity logs. The formation water resistivity is obtained by resistivity-porosity schemes or by chemical analysis or by the curve of self-spontaneous log (SP) [25]. In the present study, R_w was determined from the Basra oil data while R_{mf} was determined by the report fixed at the header of the logs, but it is necessary to make correction for the mud filtrate resistivity for each depth according to the Arp's equation:

$$R_{mf} @ T_f = R_{mf} @ T_s \left(\frac{T_s + 21.5}{T_f + 21.5}\right) \quad (17)$$

Where $R_{mf} @ T_f$ = resistivity of mud filtrate at formation temperature, ohm.m

$R_{mf} @ T_s$ = resistivity of mud filtrate at surface temperature, ohm.m

The formation temperature should be calculated during the process of log interpretation because formation water resistivity (R_w), mud filtrate resistivity (R_{mf}) and drilling mud resistivity (R_m). To calculate the formation temperature requires the calculation of geothermal gradient and is calculated by the following equation [16]:

$$G.G = \frac{BHT - T_s}{T_D} \quad (18)$$

Where: G.G = geothermal gradient

BHT = bottom hole temperature

T_s = surface temperature

T_D = total depth, m

Accordingly, formation temperature is calculated from the following equation:

$$T_f = (G.G * F_D) + T_s \quad (19)$$

where: T_f = formation temperature, C^o

F_D = formation depth, m

3.4 Determination of bulk volume water and hydrocarbon movability

A. Determination of bulk volume water

Bulk water volume (BVW) is defined as formation porosity multiplied by water saturation for formation. The bulk volume water is calculated using the equation below [25]:

$$BVW = S_w * \emptyset_{N.D} \quad (20)$$

If the bulk volume water (BVW) values in the uninvaded zone are constant, it means that the zone will be in the case of irreducible water saturation and therefore oil production should be free of water [16].

B. Determination of bulk volume hydrocarbon

Bulk volume hydrocarbon is calculated using the equation [25]:

$$BVH = S_h * \emptyset_{N.D} \quad (21)$$

3.5 Reservoir units of Nahr Umr Formation

In light of the interpretation of the well logs, Nahr Umr Formation was divided into three main reservoirs units[26] (Table 1, table 2, table 3, table 4, table 5 and Fig 2 to 9):

1. Upper Nahr Umr unit

2. Middle Nahr Umr unit

3. Lower Nahr Umr unit

These reservoir units are continuous along the study Wells (Fig 10 to Fig 17).

3.6 Petrophysics properties of the Nahr Umr reservoir main units:

1. Upper Nahr Umr unit: At the section A-A' (NW-SE), the effective porosity was good at Lu-43, while the remaining of the wells (Lu-032, Lu-030, Lu-038, Lu-045) were the effective porosity of the poor type. As for hydrocarbon saturation, it was Lu-040 (0.21), Lu-032 (0.00), Lu-030 (0.07), Lu-038 (0.04), Lu-045 (0.09). The shale volume was high at Lu-030 (0.85) in the direction SE, but when in the direction NE the shale volume decreases as follows: Lu-032 (0.58), Lu-030 (0.50), Lu-038 (0.36), Lu-045(0.36). At the section B-B' (E-W) that includes wells Lu-029, Lu-0.43, Lu-042, the effective porosity was of the Poor type at the two wells Lu-029, Lu-043, and Lu-042 was of the Fair type, while the hydrocarbon saturation was as follows: Lu-029

(0.19), Lu-043 (0.10), Lu-042 (0.02). The shale volume was high in Lu-029 (0.64) at the direction E and decrease as we go west. At section C-C' (N-S), the porosity was effective in all wells (Lu-047, Lu-033, Lu- 036, Lu-043) of the poor type. As for hydrocarbon saturation, its ratio was as follows: Lu-047 (0.17), Lu-033 (0.13), Lu- 036 (0.04), Lu-043(0.10), while the volume shale was: Lu-047 (0.44), Lu-033 (0.46), Lu-036 (0.41), Lu-043(0.38). In section D-D', the effective porosity was of the Fair type in Lu-037, Lu-006, and in Lu-005 it was of the Poor type. In the case of the hydrocarbon saturation was 0.04, 0.02 and 0.32, for Lu-037, Lu-005 and Lu-006, respectively. For the shale volume was 0.51, 0.54, and 0.28 for Lu-037, Lu-005 and Lu-006, respectively.

2. Middle Nahr Umr unit: At the section A-A' (NW-SE), the effective porosity was Very Good (Lu-400 and Good (Lu-045 and Lu-030), while Lu-038 was the effective porosity of the Fair type and Lu-0.06 was poor. As for hydrocarbon saturation was Lu-032 (0.16), Lu-030 (0.55), Lu-038 (0.39), Lu-040 (0.66), Lu-045(0.57). The shale volume was as follows: Lu-032 (0.59), Lu-030 (0.36), Lu-038 (0.49), Lu-040 (0.23) Lu-045 (0.21). At the section B-B' (E-W) that includes wells Lu- 029, Lu-0.43, Lu-042, the effective porosity was Very Good (Lu-029), Good (Lu-043) and Fair (Lu-0.42), while the hydrocarbon saturation was as follows: Lu-029 (0.53), Lu-043 (0.47), Lu-042 (0.16). The shale volume was as follows: Lu-029 (0.22), Lu-043 (0.22), Lu-042 (0.36) . At section C-C' (N-S), the effective porosity was in all wells (Lu-047, Lu-033, Lu- 036, Lu-043) of the Good type. As for hydrocarbon saturation, its ratio was as follows: Lu-047(0.23), Lu-033(0.54), Lu- 036(0.25), Lu-043(0.22), while the volume shale was: Lu-047 (0.46), Lu-033 (0.24), Lu-036 (0.39), Lu-043(0.22). In section D-D', the effective porosity was Fair (Lu-037 and Lu-005) and Good (Lu-006). In the case of the hydrocarbon saturation were 0.30, 0.32 and 0.68, for Lu-037, Lu-005 and Lu-006, respectively. In this section (D-D'), the porosity and hydrocarbon saturation increase as we direction from WN to ES. For the shale volume was 0.44, 0.38, and 0.52 for Lu-037, Lu-005 and Lu-006, respectively.

3. Lower Nahr Umr unit: At the section A-A' (NW-SE), the effective porosity was Very Good (Lu-040), Fair (Lu-038 and Lu- 045) and Poor (Lu-032). As for the hydrocarbon saturation was Lu-032 (0.00), Lu-030 (0.18), Lu-038 (0.21), Lu-040 (0.21), Lu-045(0.23). The shale volume was as follows: Lu-032 (0.27), Lu-030 (0.43), Lu-038 (0.34), Lu-040 (0.26) Lu-045 (0.30). At the section B-B' (E-W) that includes wells Lu- 029, Lu-0.43, Lu-042, the effective porosity was Excellent (Lu-029), Fair (Lu-043) and Good (Lu-0.42), while the hydrocarbon saturation was as

follows: Lu-029 (0.11), Lu-043 (0.02), Lu-042 (0.03). The shale volume was as follows: Lu-029 (0.04), Lu-043 (0.28), Lu-042 (0.18). At section C-C' (N-S), the effective porosity was in all wells (Lu-047, Lu-033, Lu- 036, Lu-043) of the Good type. As for hydrocarbon saturation, its ratio was as follows: Lu-047 (0.02), Lu-033 (0.26), Lu- 036 (0.02), Lu-043 (0.02), while the volume shale was: Lu-047 (0.22), Lu-033 (0.25), Lu-036 (0.27), Lu-043 (0.28), in this section, Vsh increase from N to S. In section D-D', the Phi was Fair (Lu-037 and Lu-005) and Good (Lu-006). In the case of the hydrocarbon saturation were 0.14, 0.03 and 0.05 for Lu-037, Lu-005 and Lu-006, respectively. For the shale volume was 0.27, 0.30, and 0.32 for Lu-037, Lu-005 and Lu-006, respectively. In this section (D-D'), the Vsh increase as we direction from WN to ES. Finally, we can say that the best reservoir units in terms of hydrocarbon saturation and production are the middle reservoir unit (Middle Nahr Umr unit).

Table 1: Classification of porosity according to Leverson (1967)

Porosity Ø (%)	Type of reservoir porosity
> 15%	**Noncommercial**
5-10%	**Poor**
10-15%	**Fair**
15-20%	**Good**
20-25%	**V.good**
< 25%	**Excellent**

Table 2: The tops of the rock units to Nahr Umr Formation in Luhais oilfield.

WELLS	U. UNIT	M. UNIT	L.UNIT	
Lu- 005	2488	2561	2606	2715
Lu- 006	2483	2562	2617	2729
Lu- 007	2492	2568	2608	2722
Lu- 018	2476	2553	2601	2714
Lu- 029	2510	2587	2629	2741
Lu- 030	2480	2551	2606	2719
Lu- 031	2486	2563	2608	2728
Lu- 032	2489	2562	2626	2716
Lu- 033	2478	2548	2605	2709
Lu- 036	2490	2566	2619	2723
Lu- 037	2493	2565	2606	2719
Lu- 038	2475	2547	2603	2705
Lu- 039	2483	2557	2620	2709
Lu- 040	2482	2559	2604	2727
Lu- 041	2479	2552	2618	2728
Lu- 042	2497	2574	2631	2736
Lu- 043	2488	2569	2618	2733
Lu- 044	2483	2566	2610	2724
Lu- 045	2497	2571	2625	2749
Lu- 046	2497	2573	2622	2743
Lu- 047	2484	2566	2610	2715
Lu- 048	2490	2558	2616	2715

Table 3: The average of logs data for the Lu–005, Lu-006, Lu-018, Lu-029, Lu-030, Lu-031, Lu-032.

			Logs												
LU - 005	Units	Thickness	CAL	GR	SN	RT	MLL	NPHI	RHOB	DT	BVW	PHI	SWT	VSH	Sh	BVh
			IN	GAPI	OHMM	OHMM	OHMM	V/V	G/C3	US/F	V/V	V/V	V/V	V/V	V/V	V/V
	Upper	73	9.20	58.47	4.05	1.85	5.18	0.28	2.38	81.26	0.08	0.08	0.97	0.54	0.02	0.00
	Middle	45	8.60	47.25	9.20	7.78	7.07	0.28	2.29	84.97	0.07	0.15	0.65	0.38	0.32	0.07
	Lower	109	9.02	37.25	4.46	3.74	24.65	0.26	2.33	77.36	0.13	0.14	0.87	0.30	0.03	0.01
			Logs													
LU - 006	Units	Thickness	CAL	GR	SN	RT	MLL	NPHI	RHOB	DT	BVW	PHI	SWT	VSH	Sh	BVh
			IN	GAPI	OHMM	OHMM	OHMM	V/V	G/C3	US/F	V/V	V/V	V/V	V/V	V/V	V/V
	Upper	79	6.23	35.63	3.39	3.16	4.74	0.23	2.45	77.28	0.07	0.11	0.73	0.28	0.32	0.05
	Middle	55	5.91	31.42	40.20	49.55	4.93	0.25	2.29	83.36	0.06	0.19	0.35	0.24	0.68	0.13
	Lower	112	6.18	36.41	2.21	1.74	1.91	0.29	2.39	77.37	0.12	0.16	0.76	0.29	0.05	0.01
			Logs													
LU - 007	Units	Thickness	CALI	GR	IND	MLL	NPHI	RHOB	SFLA	BVW	PHIE	PHIT	SWT	VSH	Sh	BVh
			IN	GAPI	OHMM	OHMM	V/V	G/C3	OHMM	V/V	V/V	V/V	V/V	V/V	V/V	V/V
	Upper	76	9.49	56.81	3.51	4.49	0.28	2.33	5.87	0.06	0.09	0.30	0.82	0.51	0.07	0.01
	Middle	40	9.54	62.81	8.46	5.02	0.30	2.19	9.29	0.06	0.12	0.33	0.71	0.52	0.34	0.07
	Lower	114	8.77	39.54	0.44	3.33	0.27	2.34	1.43	0.10	0.13	0.26	0.86	0.32	0.28	0.07
			Logs													
LU - 018	Units	Thickness	CALI	GR	MSFL	RT	SFL	NPHI	RHOB	DT	BVW	PHI	SWT	VSH	Sh	BVh
			IN	GAPI	OHMM	OHMM	OHMM	V/V	G/C3	US/F	V/V	V/V	V/V	V/V	V/V	V/V
	Upper	77	9.19	45.53	5.31	3.67	5.37	0.25	2.42	80.55	0.05	0.10	0.75	0.39	0.14	-13.86
	Middle	48	8.51	49.53	4.35	11.28	4.28	0.27	2.32	86.69	0.03	0.13	0.47	0.40	0.58	0.12
	Lower	113	8.42	32.72	1.81	2.87	1.82	0.25	2.44	76.16	0.13	0.13	0.92	0.25	0.01	0.00
			Logs													
LU - 029	Units	Thickness	CALS	GR	MSFL	ILD	ILM	NPHI	RHOB	DT	BVW	PHI	SWT	VSH	Sh	BVh
			IN	GAPI	OHMM	OHMM	OHMM	V/V	G/C3	US/F	V/V	V/V	V/V	V/V	V/V	V/V
	Upper	77	9.58	43.84	2.95	1.97	2.46	0.24	2.28	89.27	0.04	0.11	0.76	0.64	0.19	0.05
	Middle	42	8.54	28.54	2.45	6.63	4.13	0.21	2.23	83.33	0.12	0.24	0.54	0.22	0.53	0.14
	Lower	112	13.04	13.51	18.90	0.24	0.36	0.28	1.94	77.42	0.27	0.29	0.94	0.04	0.11	0.03
			Logs													
LU - 030	Units	Thickness	CALS	GR	MSFL	ILD	ILM	NPHI	RHOB	DT	BVW	PHI	SWT	VSH	Sh	BVh
			IN	GAPI	OHMM	OHMM	OHMM	V/V	G/C3	US/F	V/V	V/V	V/V	V/V	V/V	V/V
	Upper	71	10.69	53.55	3.69	2.34	2.22	0.22	2.41	86.52	0.01	0.04	0.87	0.85	0.07	0.02
	Middle	55	8.40	33.42	4.92	71.08	8.62	0.21	2.33	87.72	0.04	0.19	0.43	0.36	0.55	0.15
	Lower	113	8.39	45.34	2.46	1.43	1.23	0.20	2.42	87.65	0.12	0.17	0.85	0.43	0.18	0.05
			Logs													
LU - 031	Units	Thickness	CALS	GR	ILD	ILM	NPHI	RHOB	DT	BVW	PHI	SWT	VSH	Sh	BVh	
			IN	GAPI	OHMM	OHMM	V/V	G/C3	US/F	V/V	V/V	V/V	V/V	V/V	V/V	
	Upper	77	8.64	51.24	2.05	2.26	0.21	2.52	80.67	0.04	0.05	0.99	0.46	0.00	0.00	
	Middle	45	8.00	40.63	16.99	7.46	0.22	2.38	71.33	0.06	0.12	0.64	0.32	0.39	0.08	
	Lower	120	8.39	45.34	1.43	1.23	0.20	2.42	87.65	0.12	0.17	0.85	0.43	0.11	0.01	
			Logs													
LU - 032	Units	Thickness	CALS	GR	MSFL	ILD	ILM	NPHI	RHOB	DT	BVW	PHI	SWT	VSH	Sh	BVh
			IN	GAPI	OHMM	OHMM	OHMM	V/V	G/C3	US/F	V/V	V/V	V/V	V/V	V/V	V/V
	Upper	73	8.83	61.93	3.94	2.49	1.57	0.20	2.51	85.04	0.03	0.03	1.00	0.58	0.00	0.00
	Middle	64	8.59	69.08	4.19	22.83	6.23	0.23	2.43	85.56	0.04	0.06	0.85	0.59	0.16	0.03
	Lower	90	9.00	33.86	15.18	22.57	5.46	0.14	2.61	71.79	0.07	0.07	0.96	0.27	0.00	0.00

Table 4: The average of logs data for the Lu-033, Lu-036, Lu-037, Lu-038, Lu-039, Lu-040, Lu-041.

LU - 033	Units	Thickness	Logs													
			CALS	GR	LLS	LLD	MSFL	NPHI	RHOB	DT	BVW	PHI	SWT	VSH	Sh	BVh
			IN	GAPI	OHMM	OHMM	OHMM	V/V	G/C3	US/F	V/V	V/V	V/V	V/V	V/V	V/V
	Upper	70	8.83	51.86	2.76	2.43	4.06	0.24	2.30	80.99	0.08	0.10	0.82	0.46	0.13	0.02
	Middle	57	8.27	31.49	26.52	27.01	4.41	0.23	2.21	82.08	0.06	0.19	0.42	0.24	0.54	0.12
	Lower	104	8.75	32.09	4.39	3.75	28.72	0.23	2.26	76.86	0.11	0.17	0.72	0.25	0.26	0.06
LU - 036	Units	Thickness	Logs													
			CALS	GR	LLS	LLD	MSFL	NPHI	RHOB	DT	BVW	PHI	SWT	VSH	Sh	BVh
			IN	GAPI	OHMM	OHMM	OHMM	V/V	G/C3	US/F	V/V	V/V	V/V	V/V	V/V	V/V
	Upper	76	9.64	44.53	3.24	2.75	3.74	0.22	2.18	85.88	0.11	0.12	0.94	0.41	0.04	0.01
	Middle	53	8.75	35.73	17.64	19.92	5.97	0.27	2.13	86.49	0.09	0.17	0.67	0.39	0.25	0.06
	Lower	104	8.45	33.89	2.89	2.28	18.69	0.28	2.24	71.30	0.16	0.18	0.89	0.27	0.02	0.00
LU - 037	Units	Thickness	Logs													
			CALS	GR	LLS	LLD	MSFL	NPHI	RHOB	DT	BVW	PHI	SWT	VSH	Sh	BVh
			IN	GAPI	OHMM	OHMM	OHMM	V/V	G/C3	US/F	V/V	V/V	V/V	V/V	V/V	V/V
	Upper	72	9.43	56.35	1.91	1.84	1.98	0.25	2.26	102.33	0.09	0.10	0.93	0.51	0.04	0.01
	Middle	41	8.68	51.08	33.54	38.75	10.43	0.25	2.26	89.46	0.05	0.12	0.66	0.44	0.30	0.06
	Lower	113	8.61	34.55	2.15	1.91	3.03	0.22	2.29	78.05	0.11	0.14	0.83	0.27	0.14	0.03
LU - 038	Units	Thickness	Logs													
			CALS	GR	LLS	LLD	MSFL	NPHI	RHOB	DT	BVW	PHI	SWT	VSH	Sh	BVh
			IN	GAPI	OHMM	OHMM	OHMM	V/V	G/C3	US/F	V/V	V/V	V/V	V/V	V/V	V/V
	Upper	72	9.08	54.82	2.45	2.37	3.13	0.26	2.35	83.01	0.07	0.09	0.88	0.50	0.09	0.01
	Middle	56	8.79	54.65	17.65	17.93	2.77	0.28	2.22	87.62	0.05	0.12	0.66	0.49	0.39	0.08
	Lower	102	8.14	40.76	1.45	1.32	7.69	0.27	2.39	77.97	0.11	0.13	0.89	0.34	0.21	0.05
LU - 039	Units	Thickness	Logs													
			CALS	GR	M2R1	M2RX	RMLL	CNCF	ZDEN	DT	BVW	PHI	SWT	VSH	Sh	BVh
			IN	GAPI	OHMM	OHMM	OHMM	V/V	G/C3	US/F	V/V	V/V	V/V	V/V	V/V	V/V
	Upper	74	10.73	45.30	1.76	1.27	1.46	0.28	2.28	85.86	0.14	0.18	0.81	0.39	0.20	0.03
	Middle	63	10.11	51.07	2.68	5.16	2.32	0.27	2.26	83.52	0.09	0.16	0.65	0.45	0.34	0.08
	Lower	89	9.55	46.05	1.10	1.49	1.12	0.26	2.38	77.12	0.15	0.18	0.87	0.39	0.32	0.08
LU - 040	Units	Thickness	Logs													
			CALS	GR	M2R1	M2RX	M2R6	CNCF	ZDEN	DT	BVW	PHI	SWT	VSH	Sh	BVh
			IN	GAPI	OHMM	OHMM	OHMM	V/V	G/C3	US/F	V/V	V/V	V/V	V/V	V/V	V/V
	Upper	77	9.32	42.69	2.75	4.45	3.24	0.26	2.35	82.83	0.08	0.18	0.59	0.36	0.21	0.05
	Middle	45	8.72	30.37	4.01	20.98	10.75	0.24	2.31	88.91	0.06	0.23	0.37	0.23	0.66	0.17
	Lower	123	10.43	32.79	1.25	2.68	2.39	0.30	2.26	80.21	0.15	0.22	0.63	0.26	0.21	0.06
LU - 041	Units	Thickness	Logs													
			CALS	GR	M2R1	M2RX	RMLL	CNCF	ZDEN	DT	BVW	PHI	SWT	VSH	Sh	BVh
			IN	GAPI	OHMM	OHMM	OHMM	V/V	G/C3	US/F	V/V	V/V	V/V	V/V	V/V	V/V
	Upper	73	9.21	47.92	2.22	3.45	2.41	0.23	77.15	2.49	0.05	0.07	0.84	0.42	0.08	0.01
	Middle	66	8.52	20.96	4.16	225.52	3.38	0.21	79.68	2.27	0.05	0.21	0.31	0.13	0.60	0.14
	Lower	110	9.23	29.19	0.94	1.86	1.50	0.26	74.89	2.32	0.14	0.16	0.87	0.22	0.02	0.00

Table 5: The average of logs data for the Lu-042, Lu-043, Lu-044, Lu-045, Lu-046, Lu-47, Lu-048.

			Logs													
LU - 042	Units	Thickness	CALS	GR	M2R1	M2RX	M2R6	CNCF	ZDEN	DT	BVW	PHI	SWT	VSH	Sh	BVh
			IN	GAPI	OHMM	OHMM	OHMM	V/V	G/C3	US/F	V/V	V/V	V/V	V/V	V/V	V/V
	Upper	77	9.13	48.18	1.42	2.41	2.09	0.23	2.40	74.49	0.08	0.09	0.96	0.42	0.03	0.00
	Middle	57	8.90	42.88	2.43	4.72	3.76	0.27	2.29	82.37	0.10	0.14	0.81	0.36	0.16	0.03
	Lower	105	11.01	25.69	0.72	1.90	1.65	0.28	2.14	77.02	0.15	0.19	0.79	0.18	0.03	0.00
			Logs													
LU - 043	Units	Thickness	CALS	GR	M2R1	M2RX	M2R6	CNCF	ZDEN	DT	BVW	PHI	SWT	VSH	Sh	BVh
			IN	GAPI	OHMM	OHMM	OHMM	V/V	G/C3	US/F	V/V	V/V	V/V	V/V	V/V	V/V
	Upper	81	9.25	44.23	1.56	1.88	1.74	0.24	2.27	86.09	0.11	0.13	0.90	0.38	0.10	0.01
	Middle	49	8.98	30.03	5.00	38.77	23.39	0.24	2.22	88.25	0.06	0.19	0.44	0.22	0.47	0.11
	Lower	115	9.54	35.45	2.13	1.99	2.01	0.24	2.31	78.36	0.13	0.15	0.90	0.28	0.02	0.00
			Logs													
LU - 044	Units	Thickness	CALS	GR	M2R1	M2RX	RMLL	CNCF	ZDEN	DT	BVW	PHI	SWT	VSH	Sh	BVh
			IN	GAPI	OHMM	OHMM	OHMM	V/V	G/C3	US/F	V/V	V/V	V/V	V/V	V/V	V/V
	Upper	83	9.72	51.02	2.18	1.95	1.89	0.24	2.35	81.21	0.08	0.10	0.93	0.45	0.03	0.01
	Middle	44	8.66	37.66	5.20	40.81	2.93	0.24	2.28	84.40	0.03	0.17	0.41	0.29	0.58	0.13
	Lower	114	9.35	36.57	1.88	2.52	3.43	0.27	2.26	77.18	0.12	0.15	0.83	0.29	0.02	0.00
			Logs													
LU - 045	Units	Thickness	CALS	GR	LLS	LLD	MSFL	NPHI	ZDEN	DT	BVW	PHI	SWT	VSH	Sh	BVh
			IN	GAPI	OHMM	OHMM	OHMM	V/V	G/C3	US/F	V/V	V/V	V/V	V/V	V/V	V/V
	Upper	74	8.60	42.57	3.28	3.08	3.06	0.21	2.43	75.84	0.06	0.09	0.84	0.36	0.09	0.01
	Middle	54	7.88	29.56	37.30	43.08	2.93	0.24	2.31	81.32	0.06	0.18	0.46	0.21	0.57	0.12
	Lower	124	8.96	37.02	3.38	3.03	6.13	0.24	2.35	78.13	0.10	0.13	0.81	0.30	0.23	0.05
			Logs													
LU - 046	Units	Thickness	CALS	GR	M2R1	M2RX	RMLL	CNCF	ZDEN	DT	BVW	PHI	SWT	VSH	Sh	BVh
			IN	GAPI	OHMM	OHMM	OHMM	V/V	G/C3	US/F	V/V	V/V	V/V	V/V	V/V	V/V
	Upper	76	9.75	49.68	1.87	3.01	2.49	0.24	2.32	76.66	0.08	0.10	0.86	0.44	0.05	0.01
	Middle	49	8.39	24.46	3.17	44.61	2.64	0.22	2.27	80.43	0.07	0.20	0.42	0.15	0.53	0.12
	Lower	121	10.23	36.41	2.86	2.45	2.66	0.29	2.23	77.05	0.13	0.15	0.82	0.29	0.02	0.00
			Logs													
LU - 047	Units	Thickness	CALS	GR	M2R1	M2RX	M2R6	CNCF	ZDEN	DT	BVW	PHI	SWT	VSH	Sh	BVh
			IN	GAPI	OHMM	OHMM	OHMM	V/V	G/C3	US/F	V/V	V/V	V/V	V/V	V/V	V/V
	Upper	82	10.11	49.80	2.07	2.23	2.02	0.26	2.23	80.81	0.09	0.11	0.89	0.44	0.17	0.03
	Middle	44	10.10	52.63	3.82	5.30	4.43	0.32	2.10	87.10	0.08	0.14	0.70	0.46	0.23	0.04
	Lower	105	8.55	29.44	1.48	1.76	1.56	0.24	2.33	77.74	0.15	0.16	0.92	0.22	0.02	0.00
			Logs													
LU - 048	Units	Thickness	CALS	GR	M2R1	M2RX	RMLL	CNCF	ZDEN	DT	BVW	PHI	SWT	VSH	Sh	BVh
			IN	GAPI	OHMM	OHMM	OHMM	V/V	G/C3	US/F	V/V	V/V	V/V	V/V	V/V	V/V
	Upper	68	9.11	59.54	2.26	3.01	2.84	0.24	2.46	77.59	0.04	0.04	0.98	0.55	0.03	0.00
	Middle	58	8.63	34.98	10.31	39.34	2.19	0.23	2.28	81.88	0.06	0.20	0.45	0.12	0.35	0.08
	Lower	99	9.01	43.45	1.31	1.27	1.57	0.23	2.38	77.13	0.11	0.11	0.97	0.36	0.02	0.00

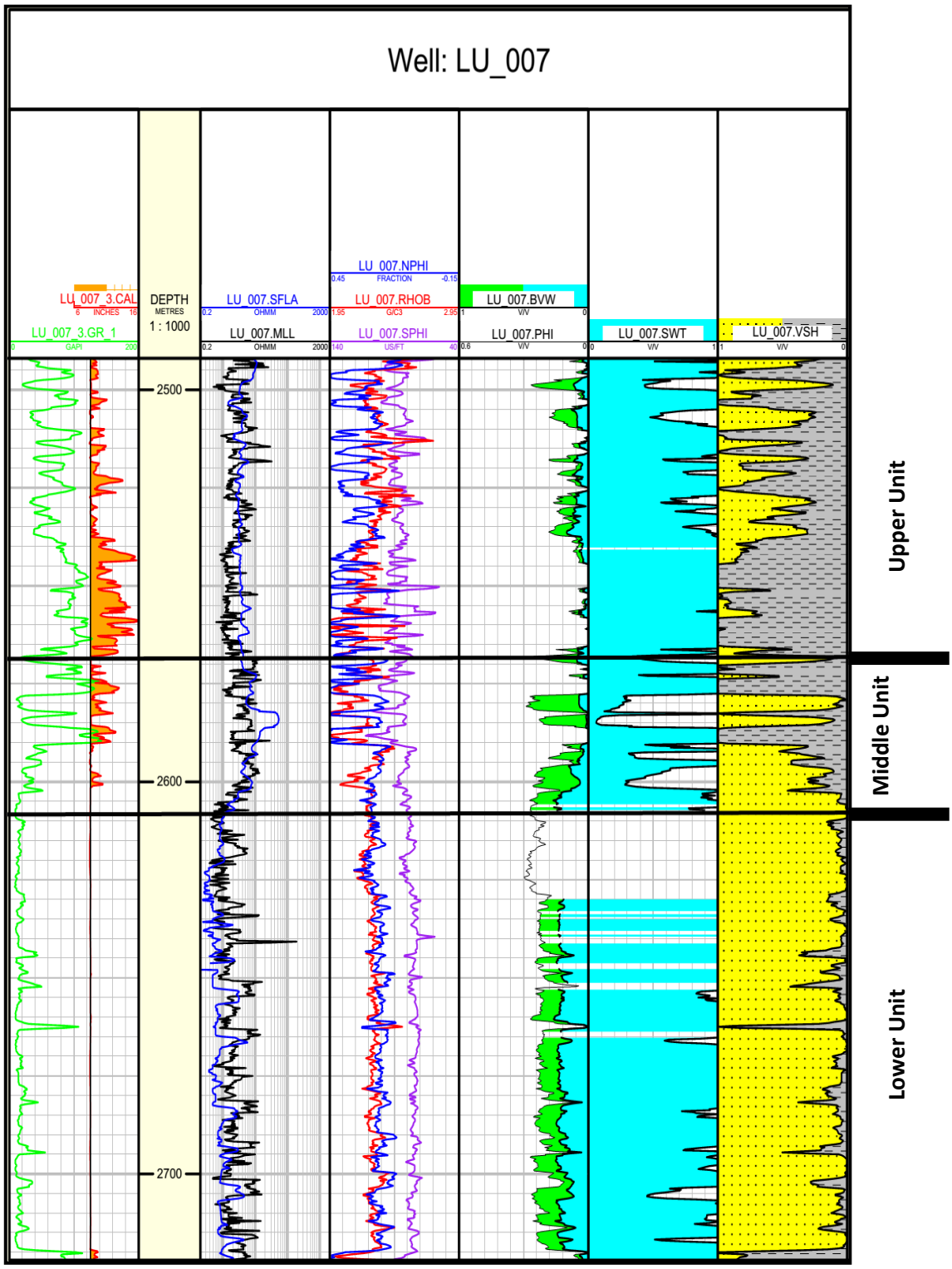

Fig. 2: Computer Processed Interpretation (CPI) of Lu-007 in Luhais oilfield (Nahr Umr Formation).

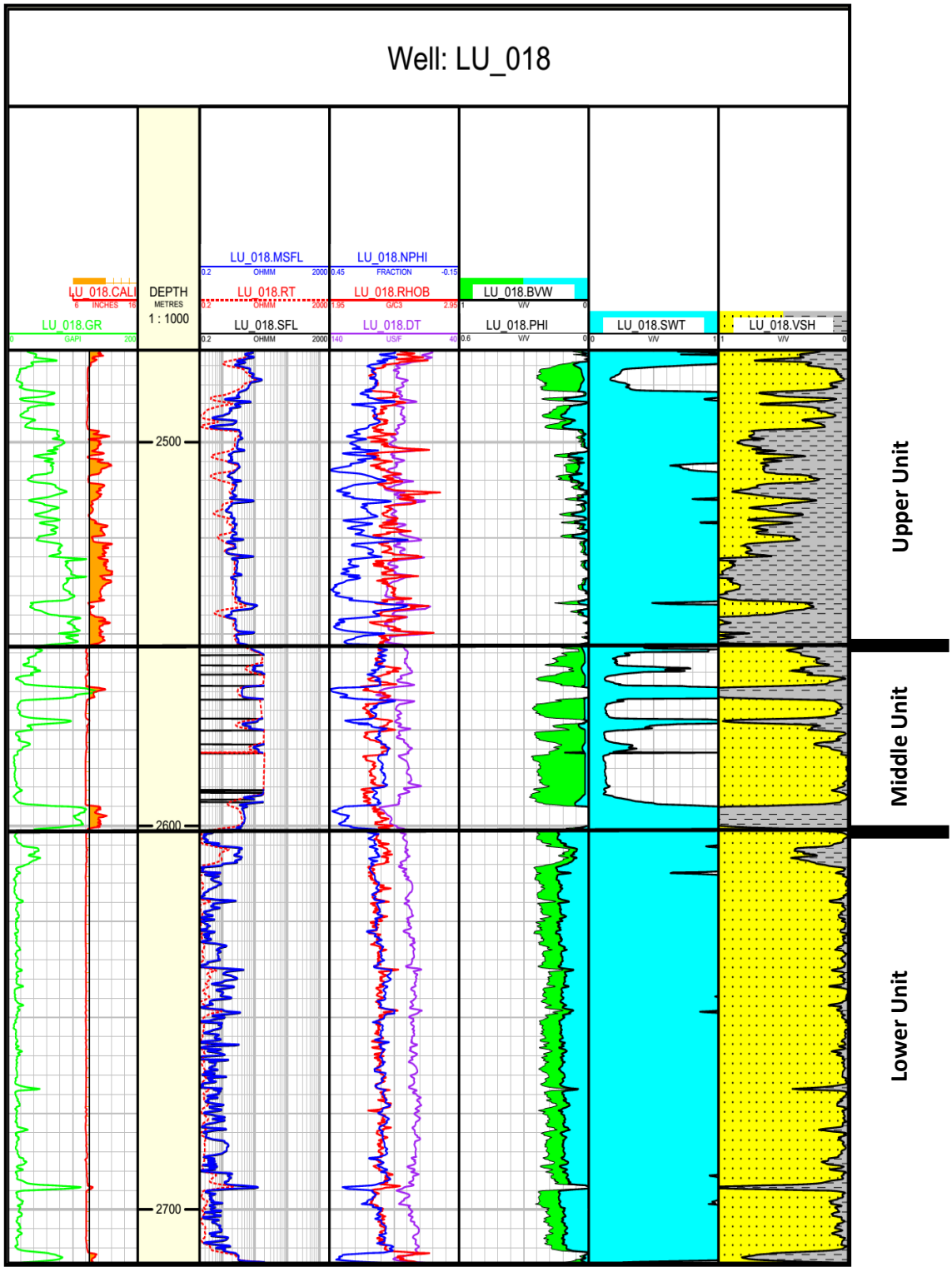

Fig. 3: Computer Processed Interpretation (CPI) of Lu-018 in Luhais oilfield (Nahr Umr Formation).

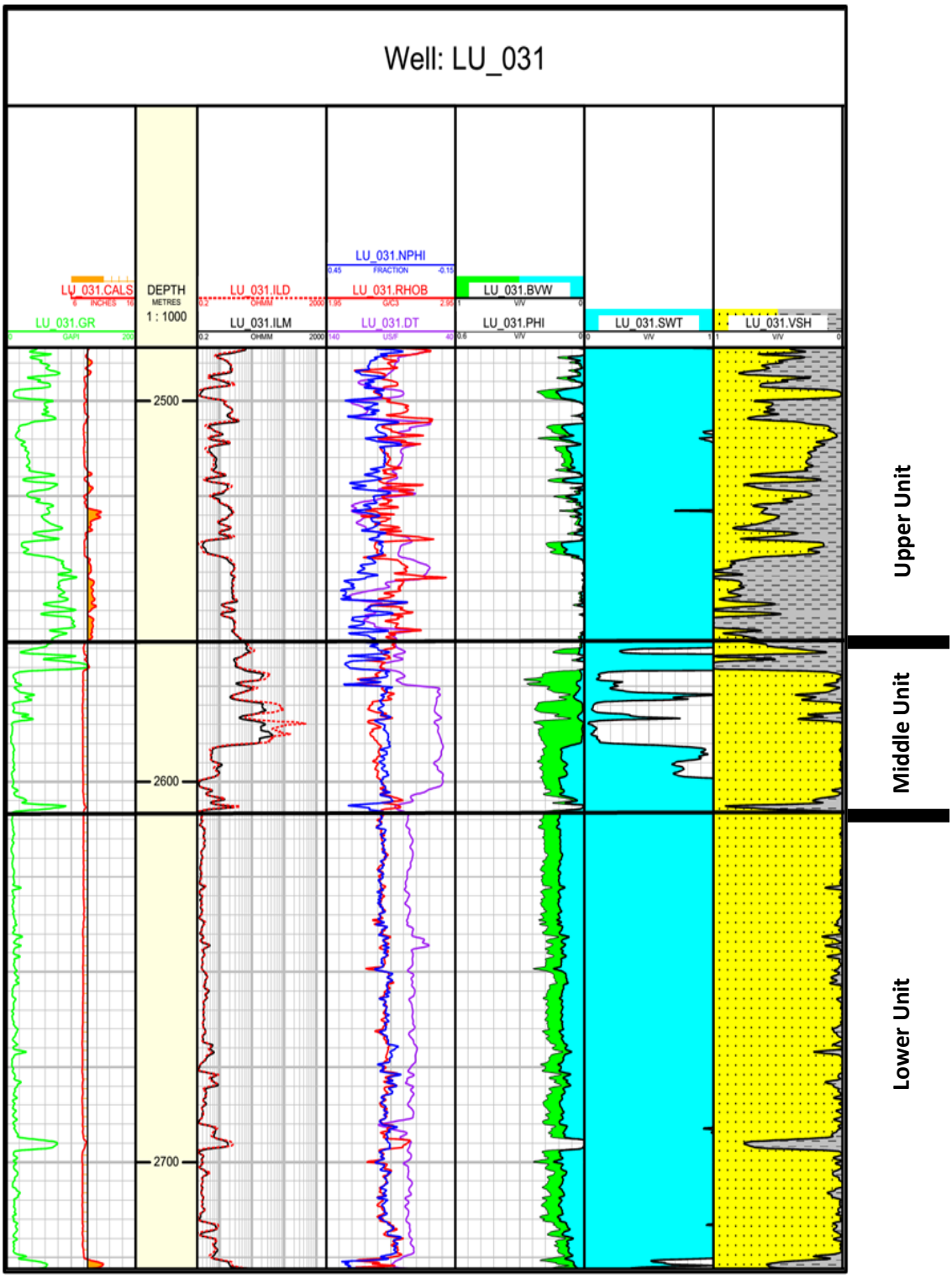

Fig. 4: Computer Processed Interpretation (CPI) of Lu-031 in Luhais oilfield (Nahr Umr Formation).

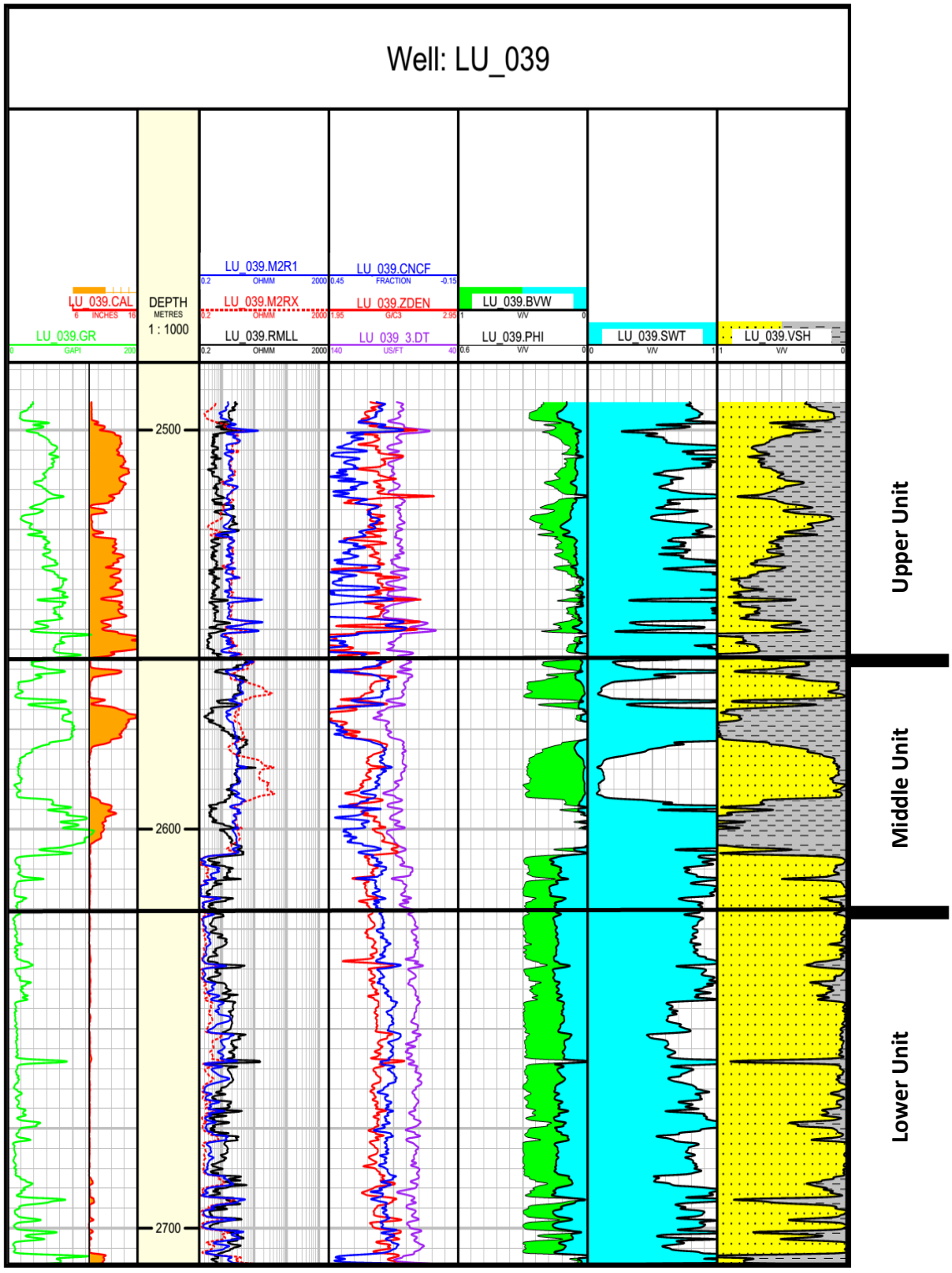

Fig. 5: Computer Processed Interpretation (CPI) of Lu-039 in Luhais oilfield (Nahr Umr Formation).

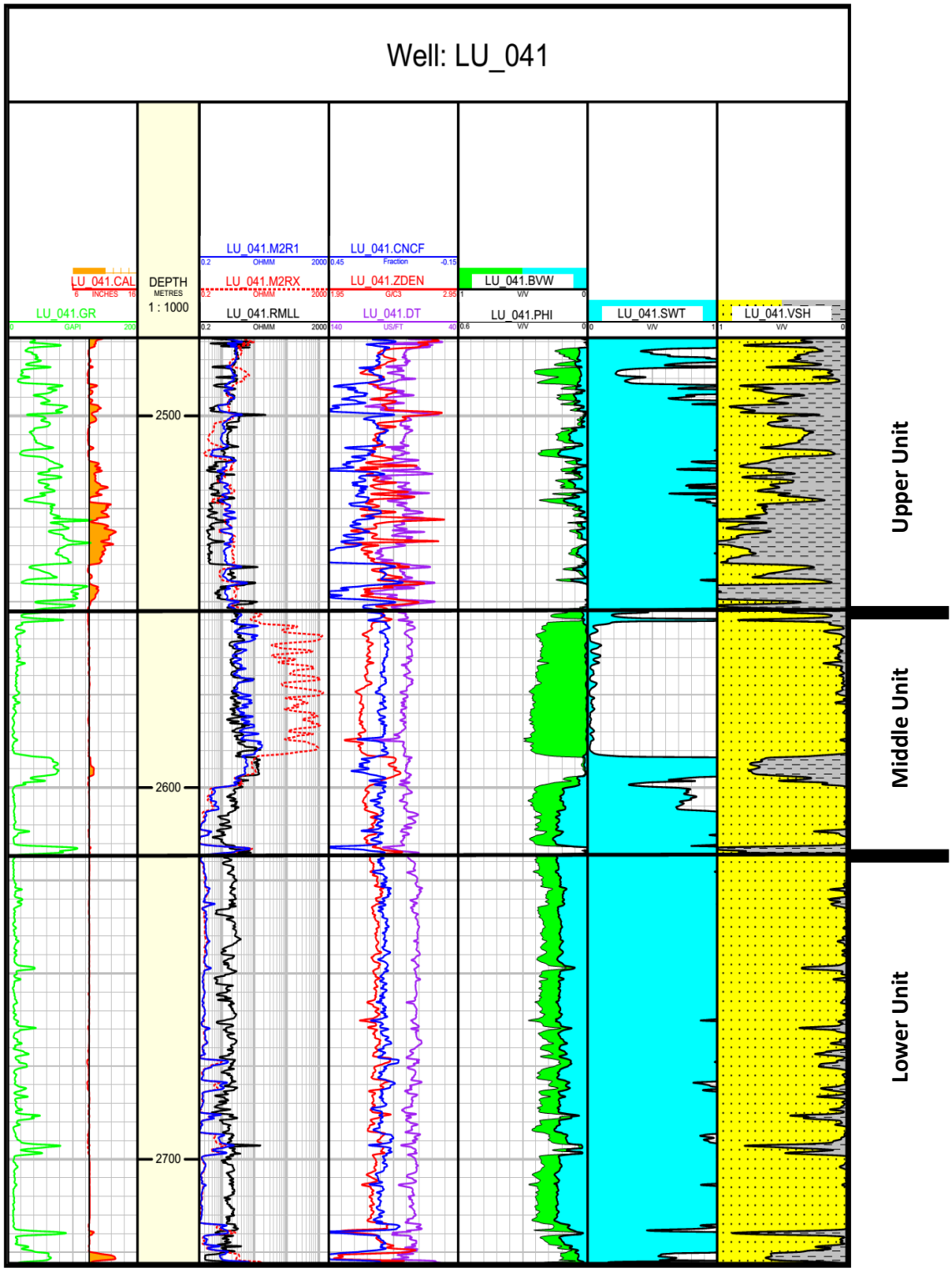

Fig. 6: Computer Processed Interpretation (CPI) of Lu-041 in Luhais oilfield (Nahr Umr Formation).

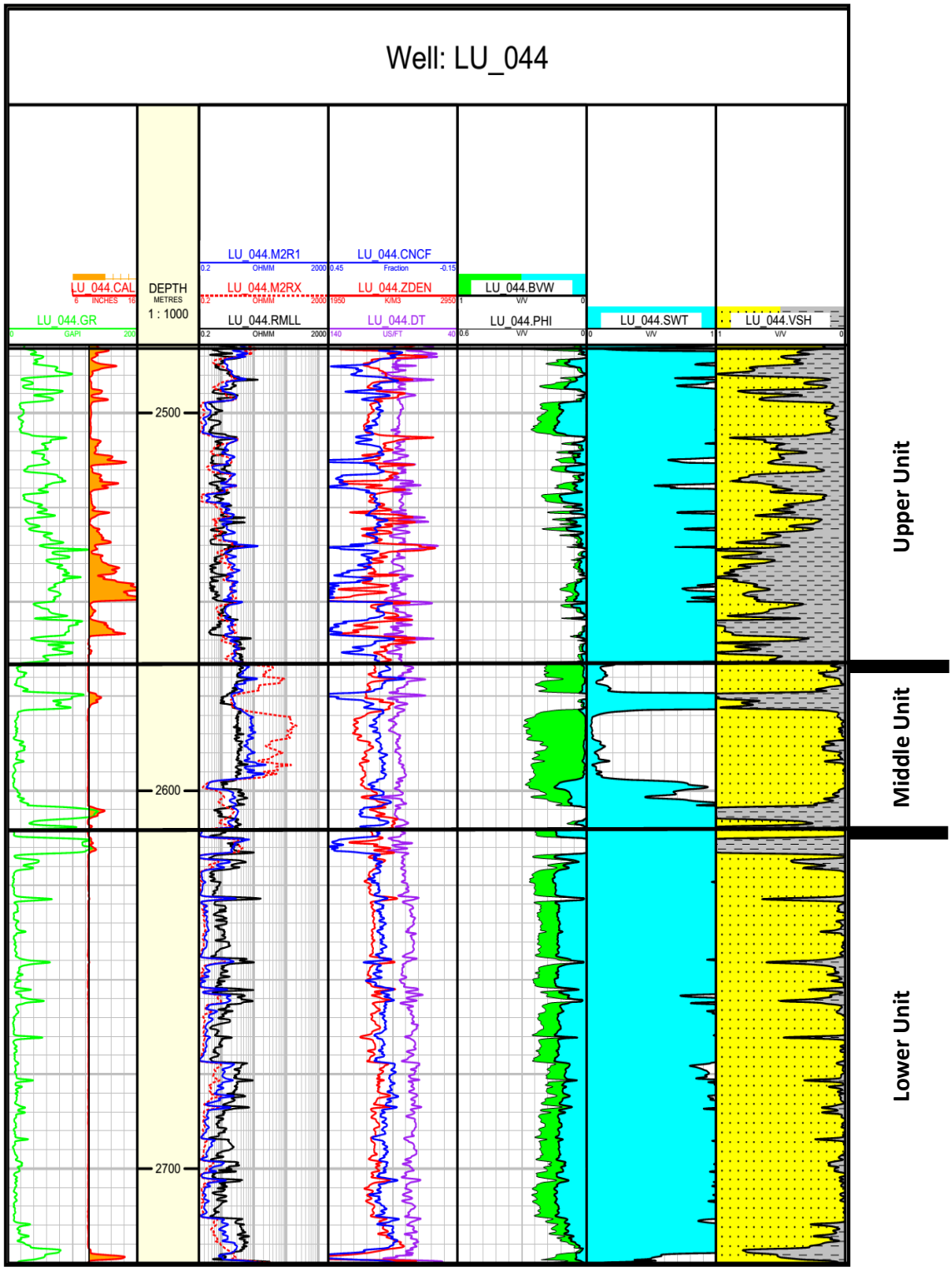

Fig. 7: Computer Processed Interpretation (CPI) of Lu-044 in Luhais oilfield (Nahr Umr Formation).

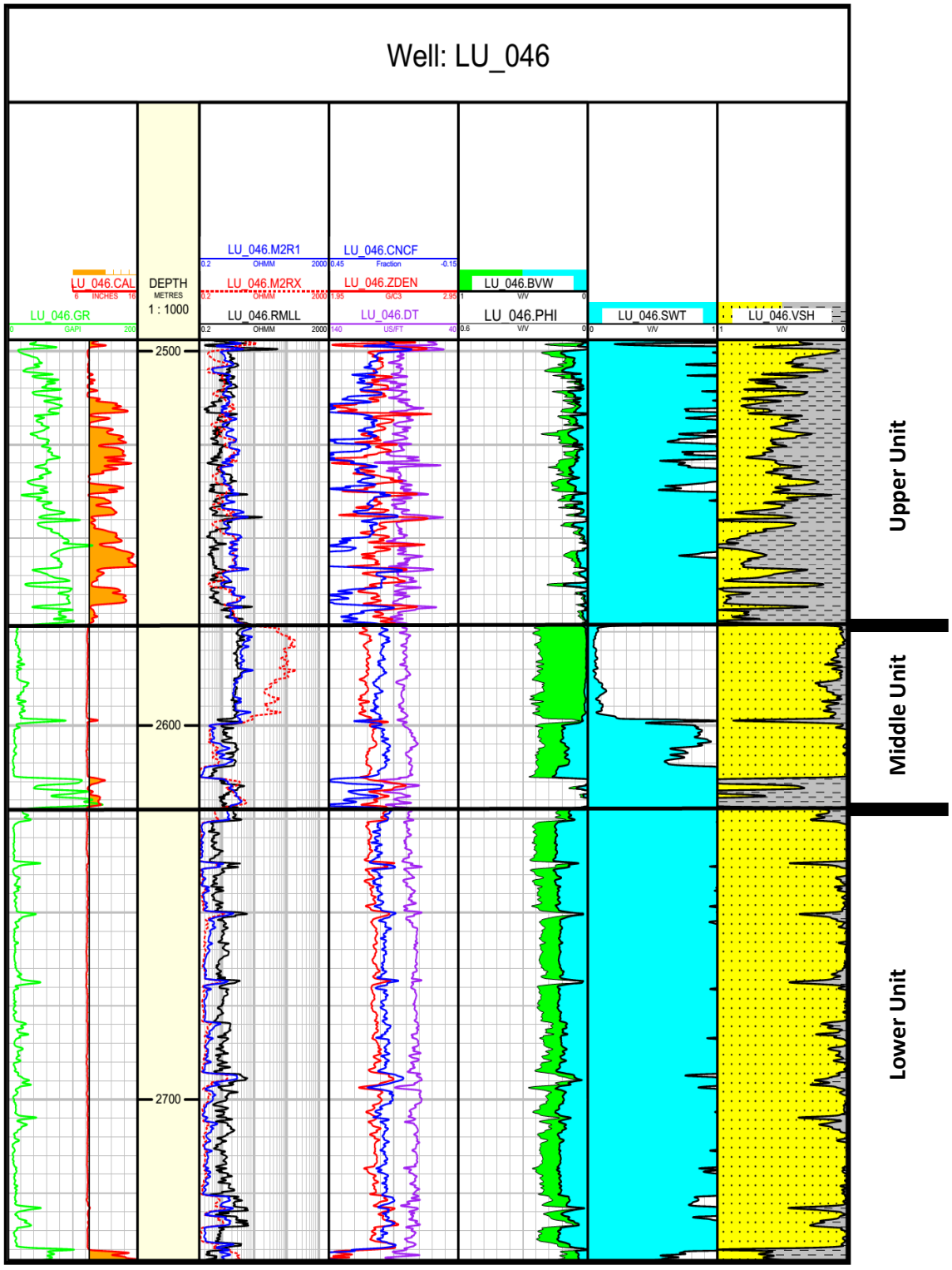

Fig. 8: Computer Processed Interpretation (CPI) of Lu-046 in Luhais oilfield (Nahr Umr Formation).

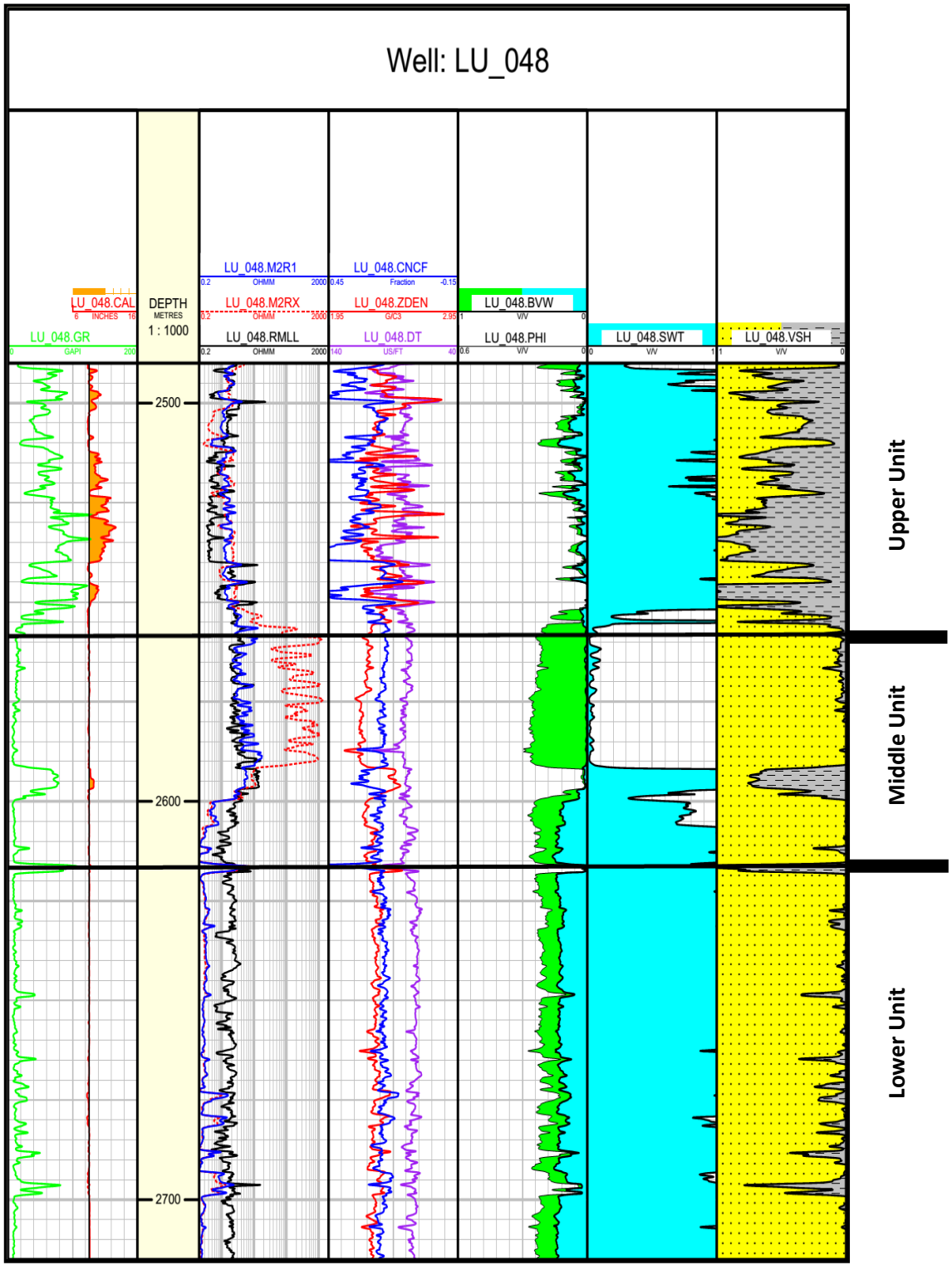

Fig. 9: Computer Processed Interpretation (CPI) of Lu-048 in Luhais oilfield (Nahr Umr Formation).

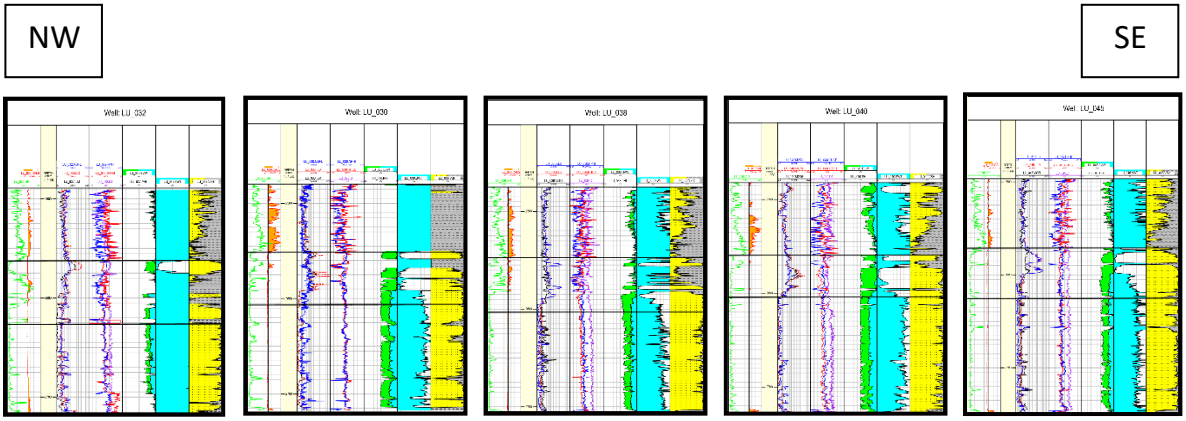

Fig. 10: Computer Processed Interpretation (CPI) of the study wells (Lu-032, Lu-030, Lu-040, Lu-045) in the direction NW-SE (Nahr Umr Formation).

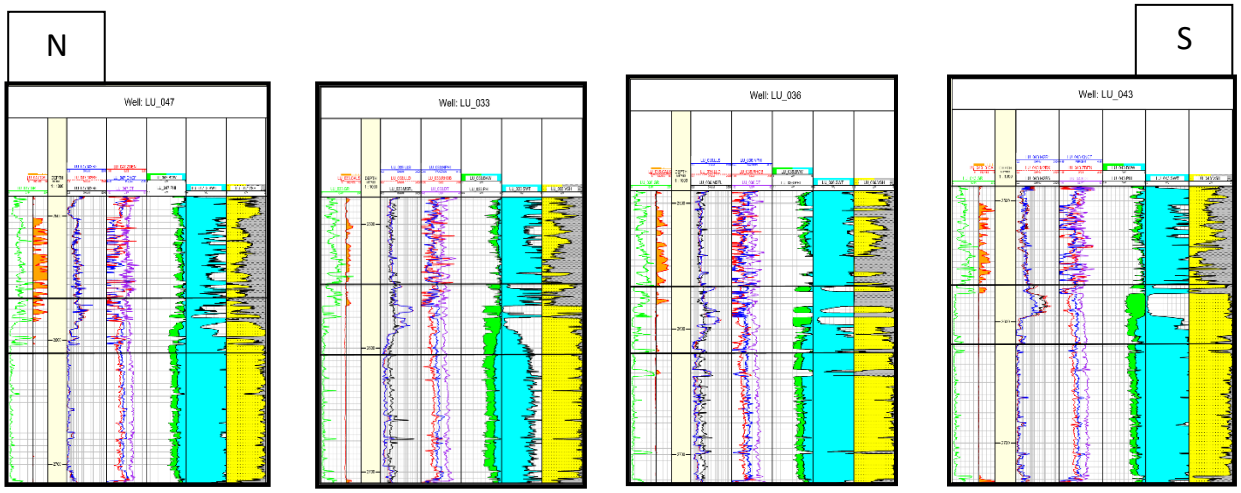

Fig. 11: Computer Processed Interpretation (CPI) of the study wells (Lu-047, Lu-033, Lu-036, Lu-043) in the direction N-S (Nahr Umr Formation).

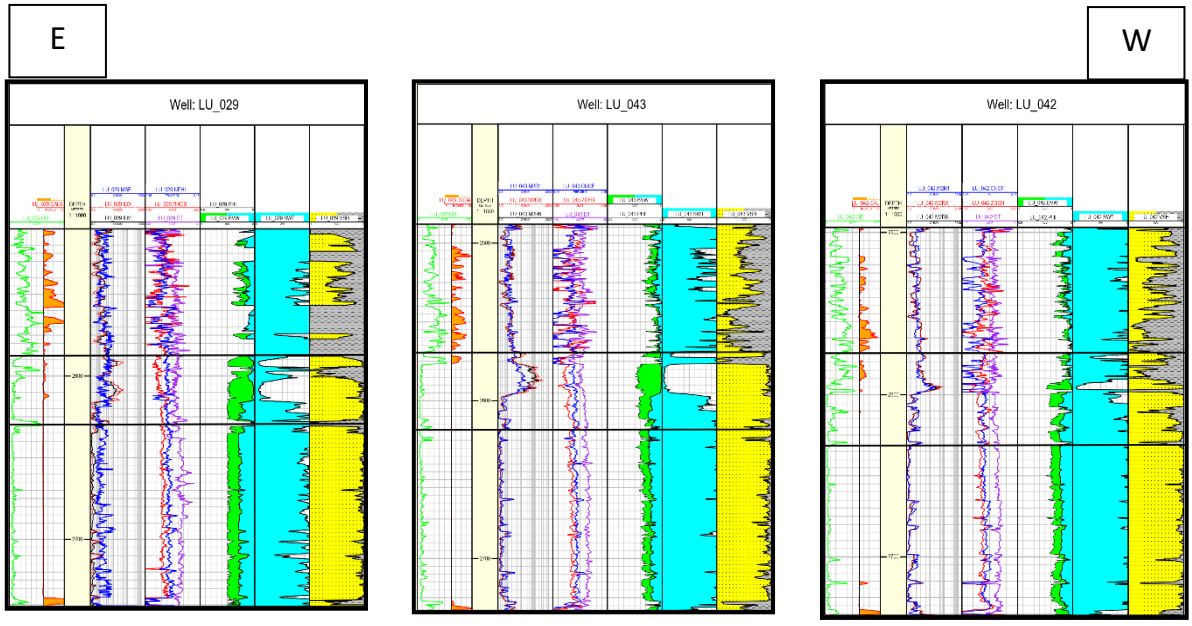

Fig. 12: Computer Processed Interpretation (CPI) of the study wells (Lu-029, Lu-043, Lu-042) in the direction E-W (Nahr Umr Formation).

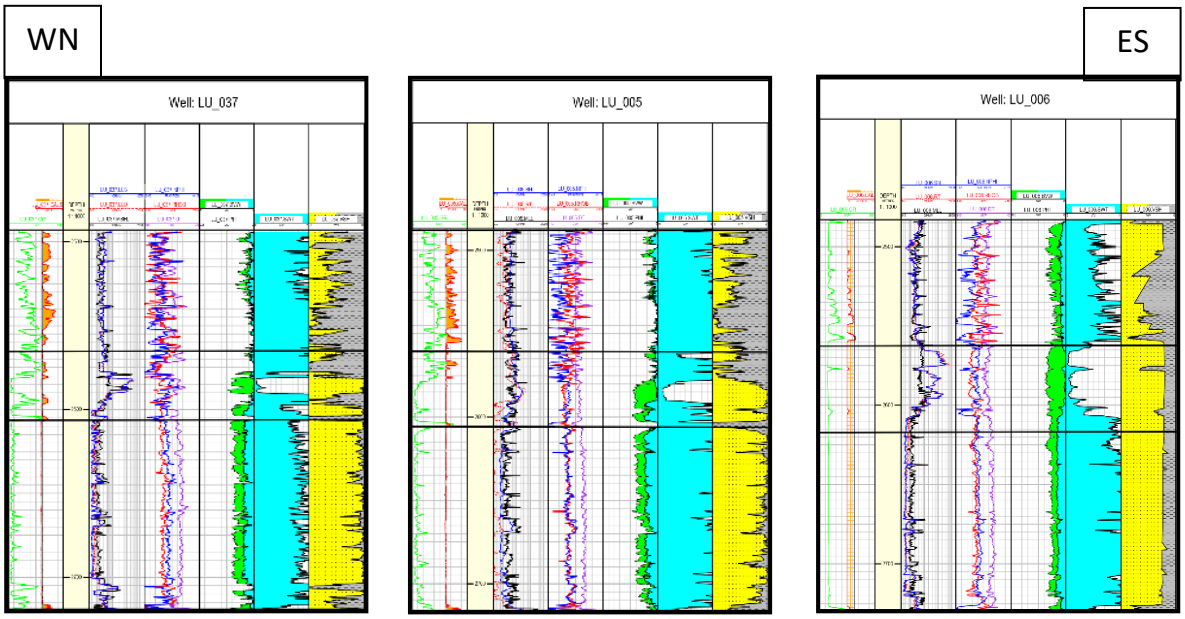

Fig. 13: Computer Processed Interpretation (CPI) of the study wells (Lu-037, Lu-005, Lu-006) in the direction WN-ES (Nahr Umr Formation).

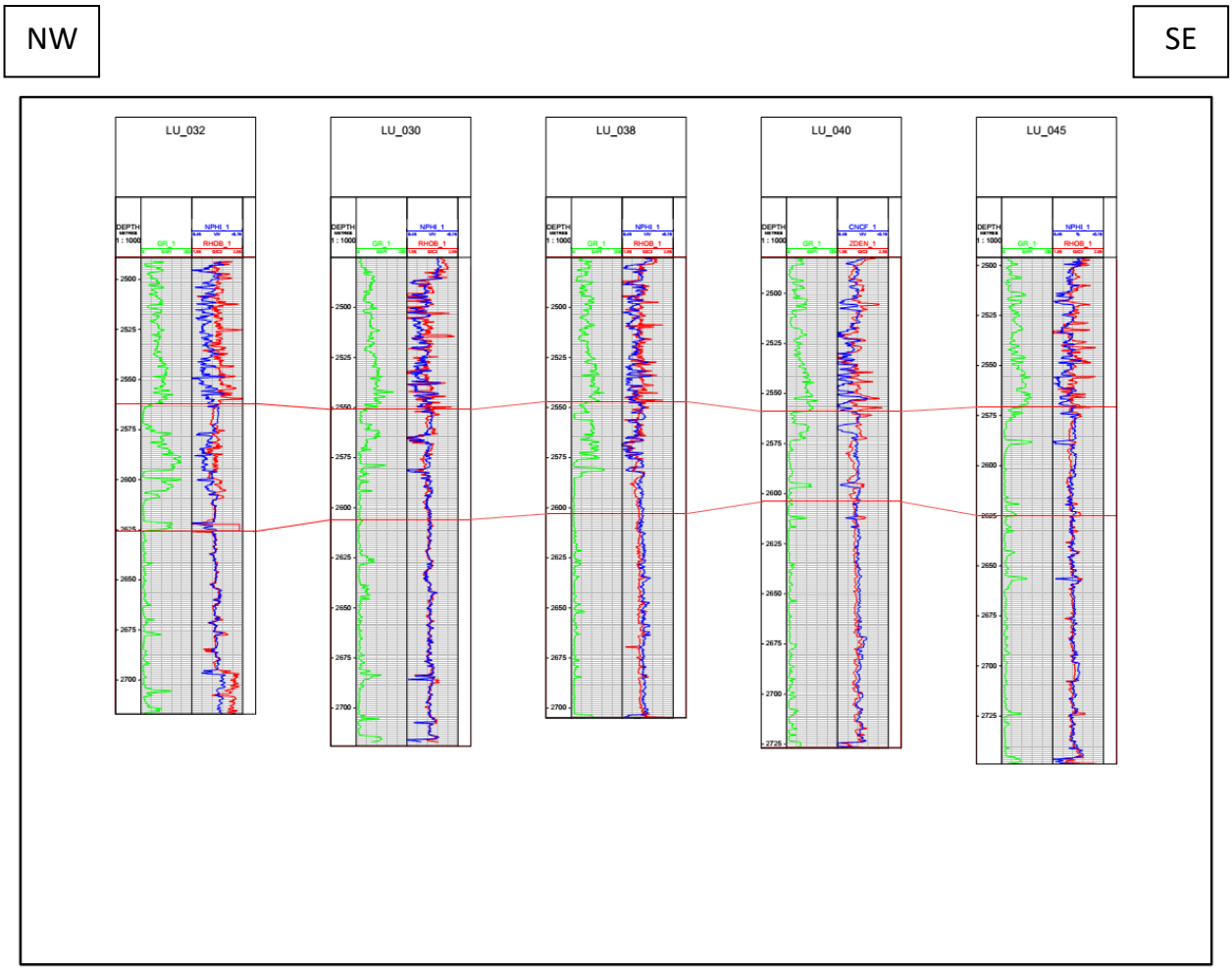

Fig. 14: Section (A-A') between the study wells (Lu-032, Lu- 030, Lu-038, Lu-040, Lu-045) in the direction NW – SE.

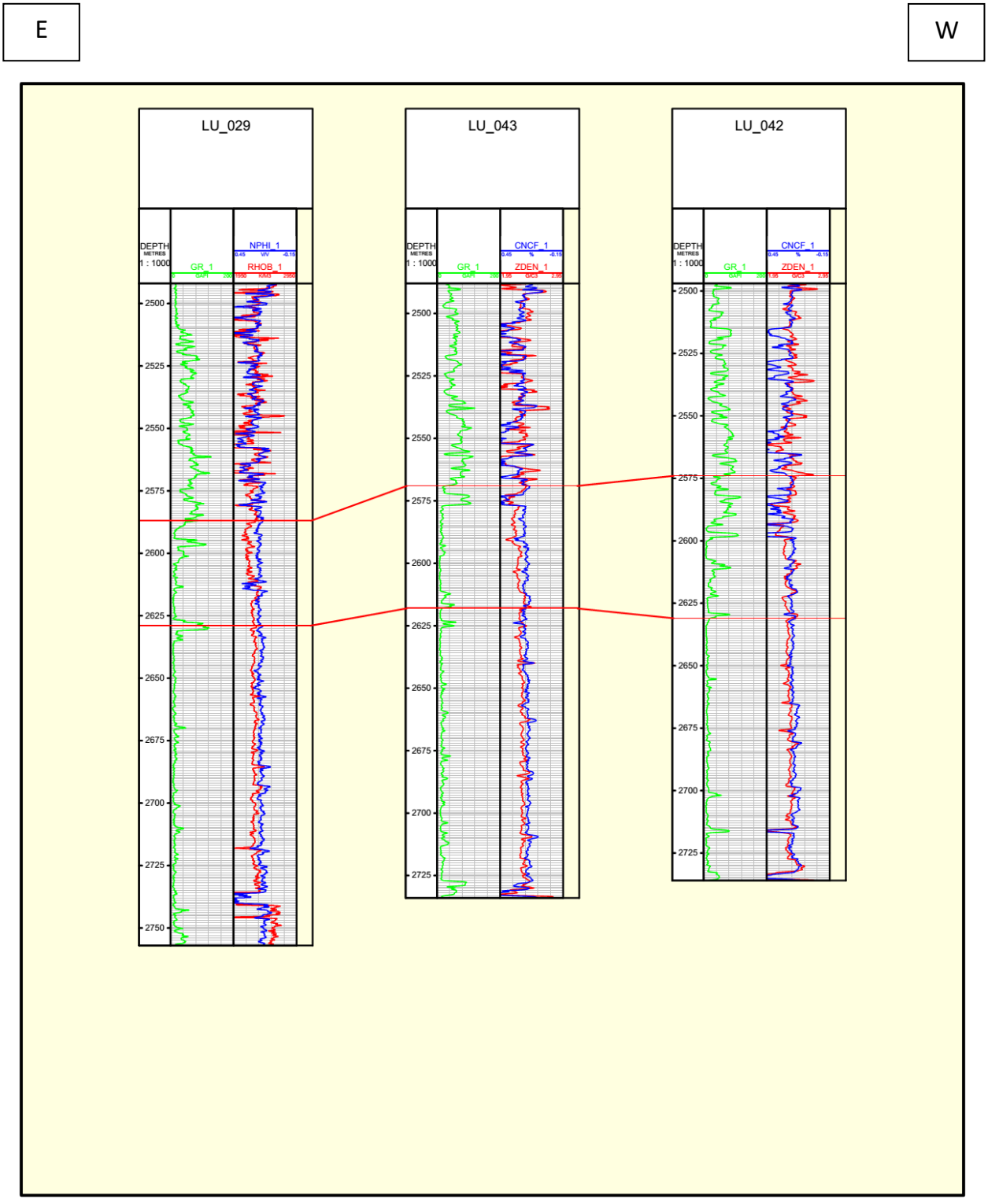

Fig. 15: Section (B-B') between the study wells (Lu-029, Lu- 043, Lu-042) in the direction E-W.

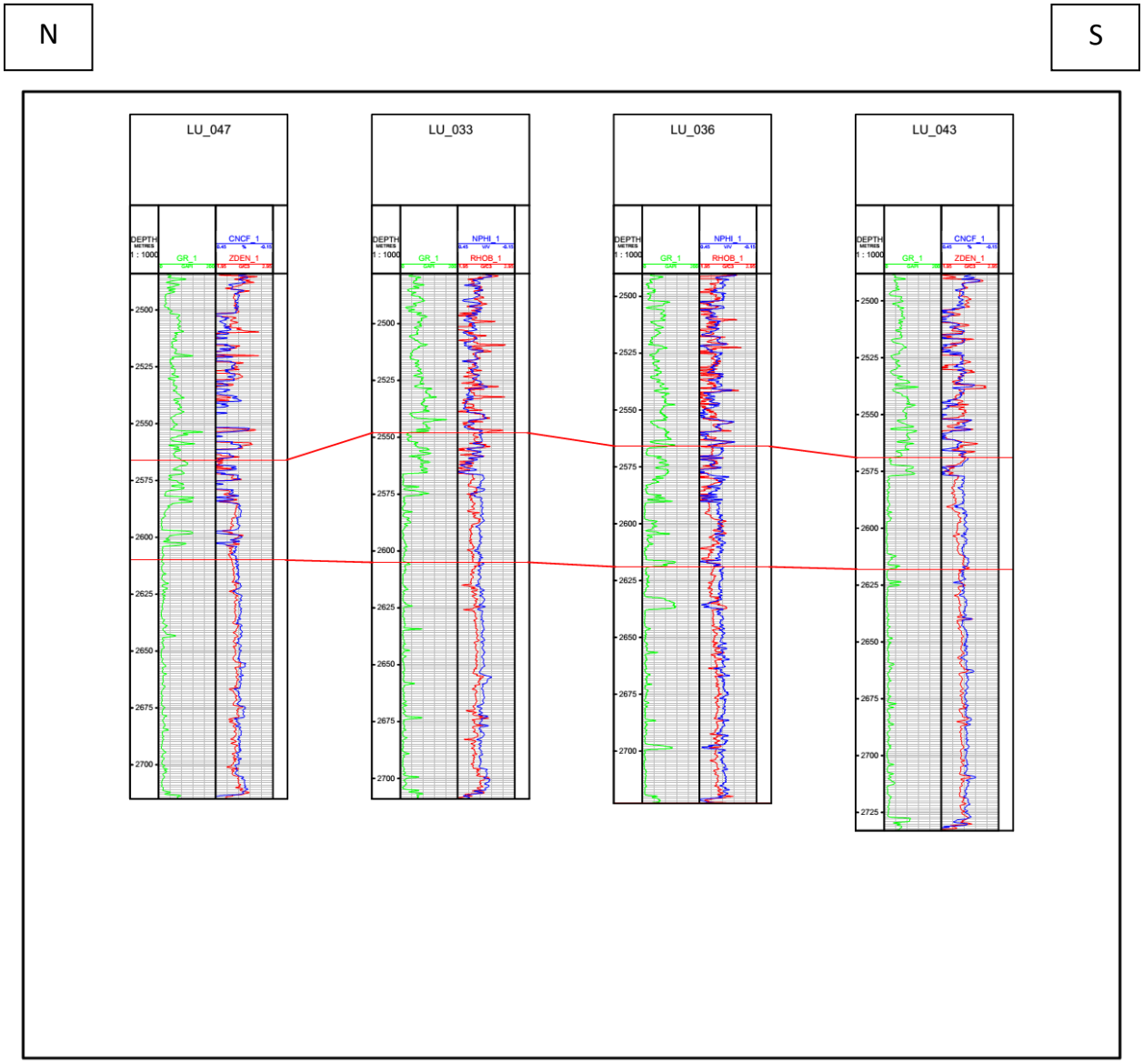

Fig. 16: Section (C-C') between the study wells (Lu-047, Lu- 033, Lu-036, Lu-043) in the direction NW-SE.

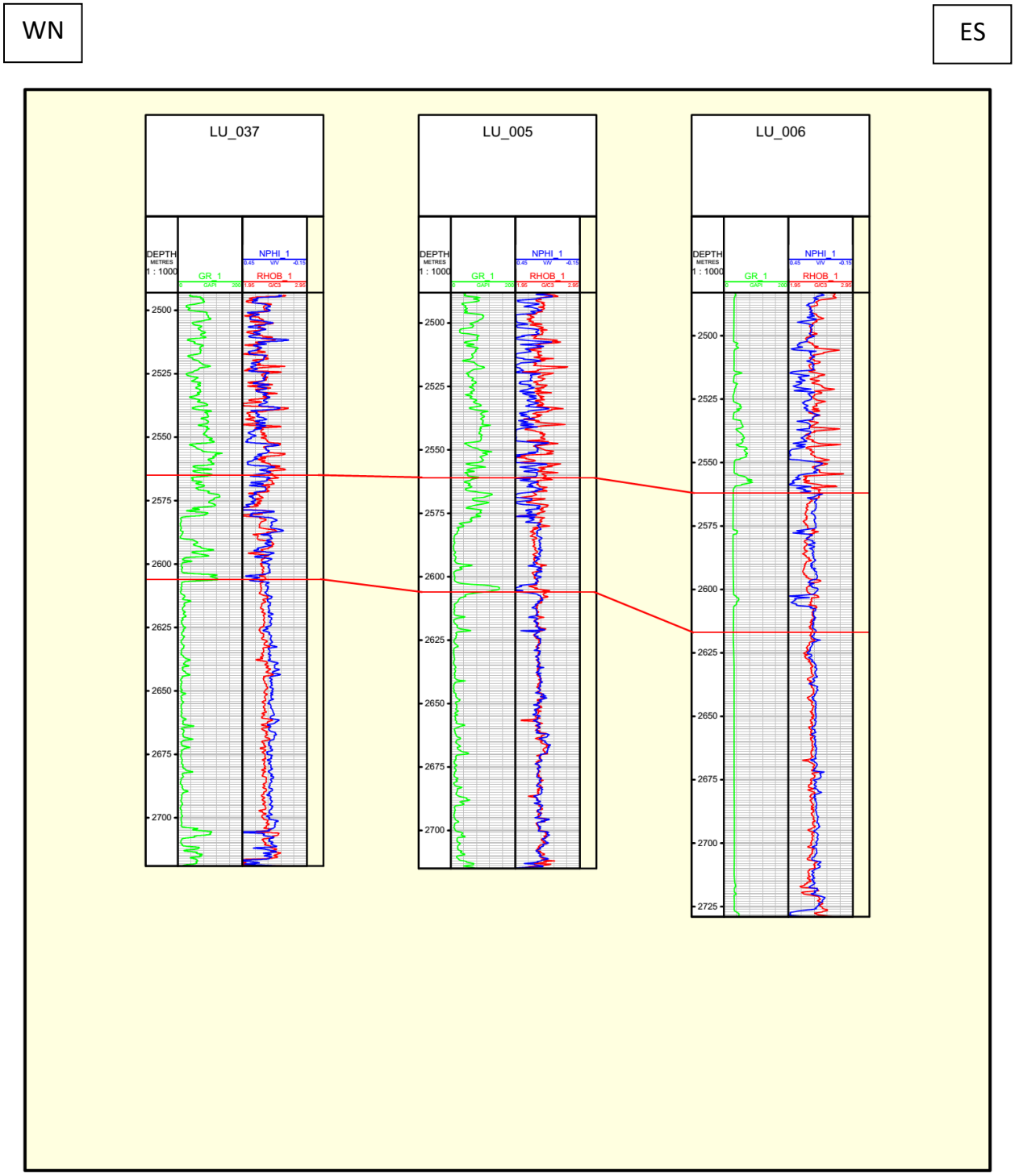

Fig. 17: Section (D-D') between the study wells (Lu-037, Lu- 005, Lu-006) in the direction WN-ES.

4. Conclusions

1. Based on the intrpretation of well logs, Nahr Umr Formation can be divided into three main reservoir units (Upper Nahr Umr reservoir unit, middle Nahr Umr reservoir unit and lower Nahr Umr reservoir unit.

2. The best of these reservoir units in most of the study wells is middle Nahr Umr reservoir unit: this reservoir unit with good petrophysical properties and producing oil.

Acknowledgments

The authors would like to thank Department of Geology, College of Science, University of Basrah, for support this research project. As well as special thanks to DR. Amna M. Handhal and Alaa M. Al-Abadi.

References

[1] R.C.V. Bellen, H. Dunnington, R. Wetzel, D. M.Morton, Lexique stratigraphique international, CNRS, Paris, 1959.

[2] R. M. Idan, F. A. Al-Musawi, A. L. Salih, S. A. Al-Qaraghuli, The petroleum system of Zubair Formation in Zubair subzone, southern Iraq, JPRS, 12 (2020) 57–73.

[3] H. A. Darweesh, , A. Z. M.Obed, , B. N. Albadran, Structural Study of Basins Configuration in Mesopotamian Area, IJEAS, 4 (2017) 54-58.

[4] S. Z. Jassim, J. C. Goff, Geology of Iraq, Dolin-Prague and Moravian museum, Brno, 2006.

[5] S. F. A. Fouad, Tectonic and structural evolution of the Mesopotamia Foredeep, Iraq, IBGM, 6 (2010) 41–53.

[6] F. H. A. Abdullah, et al., Thermal history of the Lower and Middle Cretaceous source rocks in Kuwait, GeoArabia, 2 (1997) 151–164.

[7] M. I. Husseini, The Arabian infracambrian extensional system, Elsevier, 148 (1988) 93–103.

[8] J. R. Rad et al., Basement faults and salt plug emplacement in the arabian platform in Southern Iran, J. Appl. Sci., 8 (2008) 3235–3241.

[9] A. A. M. Aqrawi, et al., Characterisation of the Mid-Cretaceous mishrif reservoir of the southern Mesopotamian Basin, Iraq, in AAPG Conference and Exhibition, 7 (2010) 7–10.

[10] N. J. Abid, , S. S. Al-Shaikhly, A. A. H. Al-Zaidy, Facies Architecture and Diagenetic Features Development of Albian-Early Turonian Succession in Luhais Oil field, Southern Iraq, IJS, 56 (2015) 2308–2320.

[11] R. M. S. Owen, S. N. Nasr, Stratigraphy of the Kuwait-Basra Area: Middle East, AAPG, (1958) 1252-1278.

[12] K. M. Al-Naqib, Geology of the Arabian peninsula: Southeastern Iraq, USGS Professional paper No., 560 (1967) 1-61 .

[13] H. V. Dunnington, , R. Wetzel, D. M. Morton, Mesozoic and Palaeozoic: Lexique stratigraphique international, Centre National de la Recherche Scientifique, 3 (1959) 1–133.

[14] M. W. Ibrahim, Petroleum geology of southern Iraq, AAPG Bulletin, 67 (1983) 97–130.

[15] P. F. Worthington, Evolution of Shaly-Sand Concept in Reservoir Evaluation, The Log Analyst, 26 (1985) 23-40.

[16] G. B. Asquith, D. Krygowski, C. R. Gibson, Basic well log analysis, Second ed., AAPG, Tulsa-Oklahoma, 2004.

[17] F. J. Lucia, Carbonate reservoir characterization: An integrated approach, Second ed., Springer, New York, 2007.

[18] M. Kennedy, Practical petrophysics, Elsevier, Amsterdam, 2015.

[19] M. R. J. Wyllie, et al., An experimental investigation of factors affecting elastic wave velocities in porous media, SEG, 23 (1958) 459-493.

[20] D. Tiab, E. C. Donaldson, Petrophysics: Theory and Practice of Measuring Reservoir Rock and Fluid Transport Properties, Fourth ed., Elsevier, Amsterdam, 2015.

[21] Schlumberger, Log interpretation charts, Schlumberger wire line & testing, Houston, 1997.

[22] G. E. Archie et.al., The electrical resistivity log as an aid in determining some reservoir characteristics, Transactions of the AIME, 146 (1942) 54-62.

[23] A. M. Handhal, A. N. Shnawa, and F. W. Majeed, Computation of cementation factor and saturation exponent for selected oil fields in southern Iraq, JPRS, 20 (2018) 113-131.

[24] Schlumberger, Log Interpretation Principle / Application, Schlumberger wire line & testing, New York, 1987.

[25] Schlumberger, Log interpretation interpretation principles / Applications, Schlumberger Wireline & Testing, 1998.

[26] Al-Garbawi, Z. H. Abady, M. F. Al-Shahwan, petrophysical evaluation for the reservoir units of Nahr-Umr formation in the Luhais oilfield south of Iraq, IGJ, 52 (2019) 83-100.

تقييم الخصائص البتروفيزيائية لتكوين نهر عمر في حقل اللحيس، جنوب العراق

باستخدام بيانات مجسات الآبار

المستخلص

يعد تكوين نهر عمر في حقل اللحيس في جنوب العراق أحد المكامن الفتاتية المنتجة التي تشكلت خلال الدورة الألبية الثانية. لتحقيق أهداف هذه الدراسة، تم أختيار اثنان وعشرون بئراً لتقييم الخصائص المكنية لتكوين نهر عمر في حقل اللحيس في جنوب العراق. تم احتساب وتفسير الخصائص البتروفيزيائية (حجم السجيل، الحجم الكلي للهيدروكاربون، التشبع الهيدروكاربوني، التشبع المائي، السماكة، الحجم الكلي للماء، المسامية) باستخدام برنامج الجيولوگ. استناداً إلى الخصائص البتروفيزيائية تم تقسيم التكوين إلى ثلاثة وحدات مكمنية رئيسية هي: الوحدة المكمنية العليا، الوحدة المكمنية الوسطى، الوحدة المكمنية السفلى. وجد بأن أفضل وحدة مكمنية من ناحية التشبع الهيدروكاربوني والأنتاج هي الوحدة المكمنية الوسطى